

Critical Capillary Absorption of Current-Melted Silver Nanodroplets into Multiwalled Carbon Nanotubes

Yen-Song Chen, Yuan-Chih Chang, Shau-Chieh Wang, Li-Ying Chen, Der-Hsien Lien, Lih-Juann Chen, and Chia-Seng Chang*

Since the discovery of carbon nanotubes (CNTs),^[1] scientists have intensively investigated their intrinsic characteristics and tried to explore their properties after combining them with other materials.^[2–15] Due to the large aspect ratio and a generically uniform diameter, the inner cavity of a CNT has been used as a nano test tube, siphon, catalyst carrier, and so on.^[4–8] Recently, CNT composites made by filling the CNTs with various materials were found to enhance the CNTs' electrical, thermal, optical, and mechanical properties;^[9–15] thus, many methods have been developed to fabricate various CNT composites. For some CNTs grown with catalysts, such as Cu and Co₉S₈, the formation of composites is usually explained by capillary action.^[16–18] Capillarity, by which the liquid is spontaneously absorbed into the narrow tube, is important for the control of channel-based devices in some biological and physical applications. The CNT is one of the smallest capillary tubes that is known on the nanoscale. Earlier studies suggest that only low-surface-tension materials can be introduced into CNTs by capillarity. This nanocapillarity has been held accountable for the various transition metals encapsulated inside the CNTs after CNT growth.^[11,16] According to recent theoretical calculations and molecular dynamics simulations, the single-walled carbon nanotube (SWCNT) with an open end can act as a “capillary pipette”, which will also absorb nonwetting metallic nanodroplets.^[19–21] Despite all these theoretical and post-factual findings, no real-time process of capillary absorption of nonwetting metal droplets by CNTs has been observed. Herein, we report the real-time capillary action of liquid Ag nanodroplets produced by electric-current heating into the CNTs. Our observation reveals that the capillary absorption of molten Ag droplets can occur only

when the ratio of the Ag droplet's size to the inner diameter of the multiwalled carbon nanotube (MWCNT) goes below a critical value, and this value decreases as the inner diameter reduces on the scale of nanometers. This finding is important for understanding the capillarity at the nanoscale and for applying it to the fabrication of CNT composites.

Figure 1a shows the transmission electron microscopy (TEM) image of one Ag nanoparticle caught by the open end of a tailored MWCNT placed on the scanning tunneling microscopy (STM) probe. The value of η is defined as the size ratio of the average Ag nanodroplet diameter D_i to the inner diameter D_t of the MWCNT. A sequence of images recording the in situ uptake behavior of a Ag droplet for the case of the initial η equal to 1.62 during electric-current heating are displayed in Figure 1a–d. The values of electric current applied at each stage are shown in Figure 1e. The chosen Ag nanoparticle was brought into contact with the upper carbon

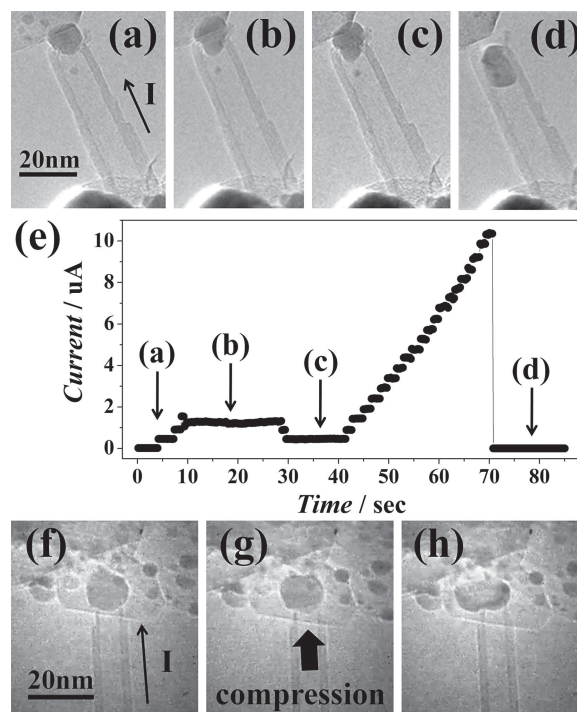


Figure 1. a–d) The dynamical process of a Ag nanodroplet being drawn into the MWCNT. The direction of current is from the STM probe to the carbon onion. e) Elapse of the passing current during the heating process corresponding to (a)–(d). f–h) No absorption occurred even with the application of mechanical compression on the Ag droplet.

Y.-S. Chen, Dr. Y.-C. Chang, S.-C. Wang, L.-Y. Chen,
D.-H. Lien, Prof. C.-S. Chang
Institute of Physics, Academia Sinica
Nankang, Taipei 11529, Taiwan
E-mail: jasonc@phys.sinica.edu.tw
Y.-S. Chen, L.-Y. Chen, Prof. C.-S. Chang
Department of Physics
National Taiwan University
Taipei 10617, Taiwan
S.-C. Wang, Prof. L.-J. Chen
Department of Materials Science and Engineering
National Tsing-Hua University
Hsinchu 30013, Taiwan



DOI: 10.1002/sml.201200393

onion in Figure 1a. When the applied voltage reached 0.03 V with a current of 1.54 μA , the Ag nanodroplet deformed and then partly entered into the MWCNT (Figure 1b). To verify that the insertion of the droplet was not caused by compression, we pulled the MWCNT containing the Ag droplet slightly away from the upper carbon onion (Figure 1c), which resulted in a decrease of current (Figure 1e). When current injection for heating the Ag nanoparticle increased to 10.37 μA , corresponding to a current density of $5.87 \times 10^6 \text{ A cm}^{-2}$, the molten Ag droplet was quickly drawn into the hollow core of the MWCNT. The Ag droplet was surrounded completely by the MWCNT and, though its shape changed, its mass remained intact. The apparent gap separating the carbon onion and MWCNT in Figure 1d implies that the speculated compression between them did not occur in the Ag absorption. To further corroborate this account, we chose to intentionally press a larger molten Ag droplet on a CNT ($\eta \approx 1.9$) as shown in Figure 1f–h, and indeed found no absorption even if the droplet was severely deformed (Figure 1h). The compression force can be estimated from the areal change of the Ag droplet under stress and the surface tension for the Ag droplet, which is 966 mN m^{-1} at the melting temperature.^[22] With the displacement of the droplet measured along the pressed direction, that is, 3.6 nm, the calculated force is roughly 9.1 nN.

In the above-mentioned experiment, the absorption of Ag nanodroplets might have been due to other effects such as: 1) the electromigration effect of electronic flow, which may promote the motion of the Ag droplet;^[2,5,11–13,23] 2) the electrowetting effect, in which the applied voltage changes the interfacial state between the Ag nanodroplet and the inner graphite shell of the MWCNT from nonwetting to wetting, and thus triggers capillary absorption;^[24] 3) the thermal gradient force, which induces the motion of the Ag nanodroplet toward lower-temperature environments;^[4,6,23] and 4) thermal evaporation, which vaporizes the Ag cluster into atoms and then aggregates them at another place.^[23] We will examine all of these possibilities. The first two effects would be induced spontaneously in our current-heating experiments.

To determine whether the electromigration effect dominates, the Ag nanodroplet was readily drawn into the MWCNT despite application of a reverse current of $-12.06 \mu\text{A}$ (current density of $3.01 \times 10^7 \text{ A cm}^{-2}$) as displayed in Figure 2a–c. The Ag-filled CNT structure in Figure 2c was moved into contact with another Ag nanoparticle on the larger MWCNT in Figure 2d and, with the current injection of $11.68 \mu\text{A}$ (current density of $2.92 \times 10^7 \text{ A cm}^{-2}$), the nanoparticle gradually melted and was drawn quickly into the MWCNT (Figure 2e). Both forward and reverse currents can cause the absorption, and the small difference between them implies that the electromigration effect could only have some minor contribution towards the absorption of the Ag nanodroplet. In the literature,^[25] it was found that a current density of $2.6 \times 10^8 \text{ A cm}^{-2}$ was needed to initiate the electromigration on a Ag nanobeam, which is about one order larger than our findings. With our measured current density, the potential electromigration force for each individual Ag atom can be calculated to be 7.5 pN, which corresponds to a shear stress of 84 MPa upon the whole Ag droplet.^[5] Since we have

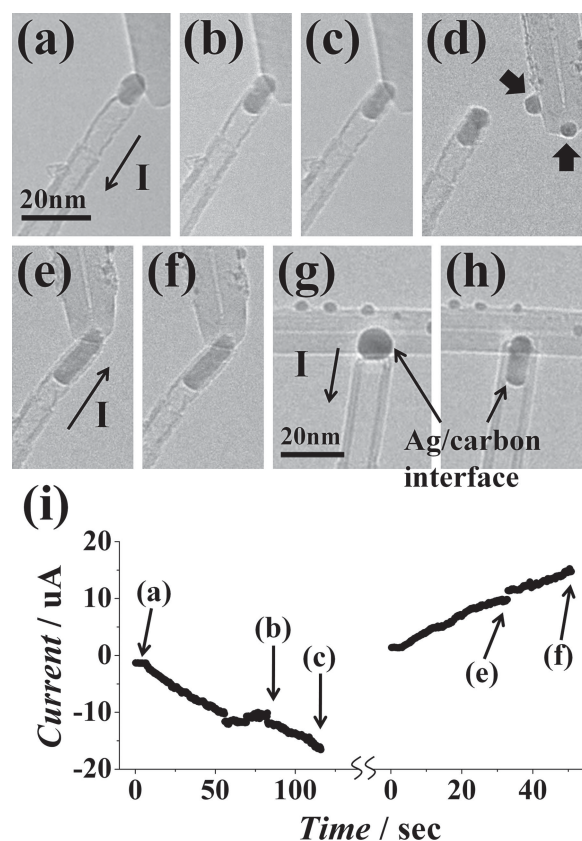


Figure 2. a–c) Absorption of a Ag nanodroplet by the tailored MWCNT with a negative current flowing from the CNT substrate to the STM probe. d) The MWCNT is then moved to another CNT containing two Ag particles. e, f) Extended absorption of Ag droplets by the MWCNT with successive uptake of two Ag particles in (d) under a positive heating current. g, h) Absorption of a Ag nanodroplet situated on a CNT by the tailored MWCNT with a negative current. The contact angle observed in (h) remains constant. i) Elapse of the passing current during the heating process corresponding to (a) to (f).

already argued that the electromigration had a minor contribution in this study, the force responsible for the absorption observed here should have a magnitude significantly larger than 84 MPa. As for the electrowetting effect, we observed in Figure 2g and h that the nonwetting condition ($\theta_c > 90^\circ$) of the Ag droplet on another CNT (before absorption) and inside the CNT (after absorption) remained unchanged while the voltage as well as current passing through the CNT were both increased. If the electrowetting effect did occur, it would be within our detection limit and can thus be considered as another minor factor in the phenomenon reported herein. Considering the thermal gradient force, the Ag nanodroplets should prefer to move away from the hottest point of a CNT, which is normally found at the contact ends or the midpoint of the tube. Although it is likely that some temperature gradient is established along the CNT crossing two electrodes, if the thermal stress played a significant role it would continue to drive the nanodroplet toward the cooler ends. This is not observed in our experiment where the nanodroplet tends to halt right after being drawn into the tube, even with a continual increase of the injection current for more than 20 s (Figure 2e, f) or even longer (Figure 2b, c). The scenario

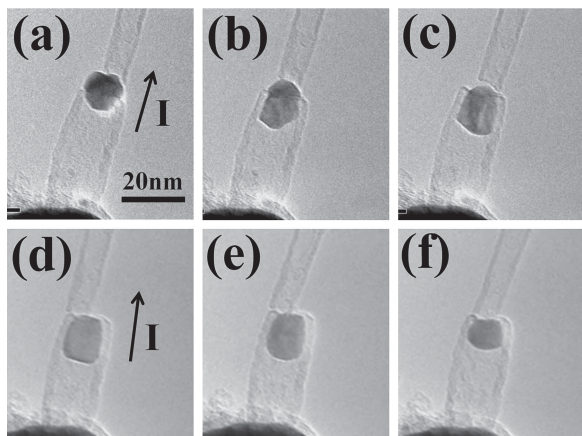


Figure 3. a–c) Absorption process of one Ag droplet contacted by two MWCNTs with different inner diameters. d–f) Shape variation of the Ag droplet inside the MWCNT as the current increased. e) The contact angle $\theta_c \approx 120^\circ$ at the interface between the molten Ag nanoparticle and the inner graphite shell of the MWCNT was obtained at currents above $10 \mu\text{A}$. f) The Ag droplet inside the MWCNT began to vanish gradually at a current of about $27 \mu\text{A}$.

shown in Figure 2e and f should help explain away the electromigration effect as well. The process of thermal evaporation did occur in our case but at much higher temperature as shown in **Figure 3f**. Once it happens, the Ag nanoparticle will gradually break away and cannot retain its original mass. Thus, the effects of thermal gradient force and evaporation contribute very little in the initial stage of the Ag nanoparticle's uptake by the CNT.

Figure 3a–c shows the absorption result of one Ag nanoparticle 12.17 nm in diameter simultaneously contacting two different MWCNTs. The inner diameters of thin and thick MWCNTs are 4.65 and 10.14 nm , respectively, and the corresponding ratios η_1 and η_2 are 2.62 and 1.20 . When the passing current reached $11.89 \mu\text{A}$, the Ag nanoparticle began to drain into the inner cavity of the thick MWCNT as shown in Figure 3b. A small drop in current led to incomplete absorption due to a loose contact resulting from the deformation of the droplet. When the contact resumed and the current was increased back to $11.79 \mu\text{A}$ (current density of $6.08 \times 10^6 \text{ A cm}^{-2}$), the Ag droplet again drained deep into the thick MWCNT and remained near its open end (see Figure 3c). These images directly demonstrate that the success or failure of the absorption is dependent on the value of η . As seen in Figure 3d and e, we connected the tubes again and continued to increase the heating current above $10 \mu\text{A}$; the contact angle $\theta_c \approx 120^\circ$ was then revealed between the molten Ag nanoparticle and the inner graphite shell of the MWCNT.^[21,26] With the amount of current $I \approx 20 \mu\text{A}$, twice as large as needed for absorption, the Ag droplet did not move in any further (see Figure 3e,f), which once again confirmed that both electromigration and thermal stress played minor roles. Finally, the Ag droplet evaporated away gradually at the current $I \approx 27 \mu\text{A}$ (see Figure 3f). The temperature at which the Ag nanoparticle melted by resistive heating could not be determined by our experimental setup. However, the changes in the Ag nanoparticle's structural phases at each stage of resistive heating were observed and could be used as a reference. When the

Ag nanoparticle melted, absorption by the CNT normally took place immediately.

In our experimental observations, the absorption mainly results from the capillary force, and the shear stress generated by this force should have a magnitude larger than 84 MPa . Unlike the macroscopic capillarity, which occurs in a tube only for the wetting liquids with $\theta_c < 90^\circ$, the capillary action at the nanometer scale depends on both the pressure difference, $\Delta P_{\text{meniscus}}$, across the meniscus of the Ag nanoparticle in the MWCNT and the Laplace pressure, ΔP_{sphere} , between the Ag droplet and the substrate.^[27] A sufficiently small nonwetting metallic droplet can thus be drawn into a CNT, and the condition for the capillary action is defined by η_c , the critical size ratio of the nanoparticle to the tube inner diameter. The value of η_c can be singly determined as $\eta = -1/\cos\theta_c$, which has been calculated as ≈ 2 for an unsupported droplet,^[19,28] if the contact angle $\theta_c = 120^\circ$ is given. However, the contact angle in the energetic term reflects the adhesion energy per unit area between the Ag droplet and the CNT, which may vary with the size of the CNT due to its curvature.

We thus performed systematic experiments to test the dependence of the value η_c on the CNT's diameter (D_t). As shown in **Figure 4a**, with each CNT of fixed inner diameter

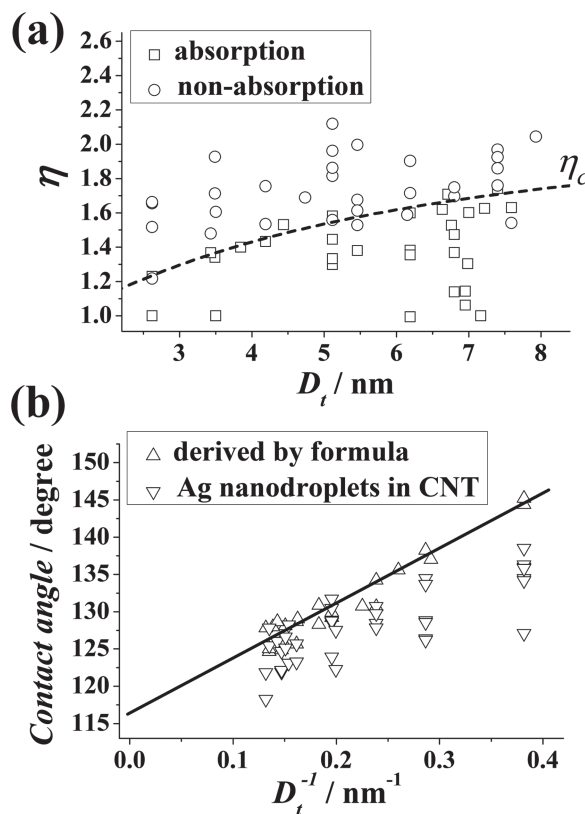


Figure 4. a) Distribution of different η ratios versus D_t . The transition from absorption (squares) to nonabsorption (circles) is observed for a specific η_c at each fixed diameter of the CNT. The critical absorption condition for Ag droplets occurs below the boundary η_c , which decreases as the diameter of the CNT reduces. b) The downward-pointing triangles represent the observed real-time contact angles in the experiment. The upward-pointing triangles are derived, using the equation $\eta = -1/\cos\theta_c$, from the experimental points near the boundary in (a). The line is a linear fit through the upward-triangle symbols.

we can change the value η by approaching various Ag droplets and the transition from absorption to nonabsorption is observed at a certain critical value (η_c). The distribution of D_t in our study spans from 2.5 to 8.0 nm. An obvious monotonically declining boundary curve, which separates the absorption from nonabsorption, was observed from the larger CNT toward the smaller size. The corresponding η_c value at the boundary ranges from 1.7 to 1.2. This experimental result clearly unveils the significance of the CNT's size for the capillary action. Once again, as evident from the absorption of nonwetting Ag droplets, it demonstrates that on the scale of several nanometers, the size-dependent nature of the capillary action of CNTs is remarkably robust. The change of the critical ratio η_c also represents the variation of the contact angle θ_c with the CNT's diameter, and an increase of contact angle suggests the reduction of adhesive energy per unit area as the CNT becomes smaller. Referring to the boundary value of η_c in Figure 4a, using the above equation we can derive the corresponding contact angle (θ_c) for each CNT diameter, values of which are depicted in Figure 4b as upward-pointing triangles versus D_t^{-1} and fitted with a straight line. This trend is expected as a result of curvature and is similar to the simulation result obtained by Kutana and Giapis,^[29] in which they showed that the contact angle of the mercury slug in the SWCNT cavity varied linearly with the inverse of CNT diameter. The measured contact angles of the droplets inside different CNTs after capillary absorption are marked in Figure 4b for comparison, and the general trend goes up with D_t^{-1} . The scattering of observed contact angles is most likely due to the instability of molten Ag droplets during current injection. However, the data derived from Figure 4a are less scattered and allude to the origin of the dependence of the critical ratio η_c on the CNT diameter.

In conclusion, we have presented in situ observations of the capillary absorption of current-melted Ag nanodroplets by tailored MWCNTs. As the ratio (η) of a droplet's size to the CNT's inner diameter goes below a critical value, the nonwetting Ag droplet can be drawn into the hollow core of the CNT through capillary action. We also found that the contact angle between a Ag droplet and a CNT inner wall increases when the inner diameter of the CNT gets smaller. This results in the dependence of the critical absorption value of η_c on the CNT's inner diameter (D_t), that is, η_c will rise monotonically with D_t when it is less than ≈ 8 nm.

Experimental Section

In situ experiments were performed in an ultrahigh-vacuum (UHV) transmission electron microscope (JEOL-2000V, working at an accelerating voltage of 200 kV and electron beam current density of about 100 pA cm⁻²) and recorded the dynamical process of nonwetting Ag nanodroplets drawn into the hollow cores of MWCNTs. The UHV-TEM system was equipped with a charge-coupled device (CCD) camera of 1 million pixels and a TV recorder. They recorded images of a capillary process at 2 and 30 frames per second, respectively. First, MWCNTs were prepared on the knife edge of a gold sheet by electrophoresis at ambient pressure. This gold sheet was then mounted on the TEM sample holder and placed into a

load-lock chamber. After the load-lock chamber was evacuated, the holder was quickly transferred to the main chamber of the UHV-TEM instrument. The TEM system was also equipped with a movable STM probe with which we first chose an individual CNT and made physical contact to establish a complete electrical circuit for heating or measurement. We also prepared suitable open-ended MWCNTs of specific diameters by extracting their inner shells for approaching different Ag droplets.^[30,31] The procedure involved the deposition of Ag atoms on the MWCNTs by a UHV electron-beam evaporator.^[32] A chosen Ag nanoparticle was then touched with the tailored open-ended MWCNT. To trigger the capillary action we needed to melt the Ag particle, which was achieved by applying a dc current to generate local heating near the particle. Here, we define the positive (negative) current referring to the STM probe as the positive (negative) electrode.

Acknowledgements

We are grateful for the support from the National Nanoscience and Nanotechnology Program of Taiwan under grant number NSC97-2120-M-001-008.

- [1] S. Iijima, *Nature* **1991**, 354, 56.
- [2] B. C. Regan, S. Aloni, R. O. Ritchie, U. Dahmen, A. Zettl, *Nature* **2004**, 428, 924.
- [3] P. M. F. J. Costa, D. Golberg, M. Mitome, S. Hampel, A. Leonhardt, B. Buchner, Y. Bando, *Nano Lett.* **2008**, 8, 3120.
- [4] L. Dong, X. Tao, L. Zhang, X. Zhang, B. J. Nelson, *Nano Lett.* **2007**, 7, 58.
- [5] K. Svensson, H. Olin, E. Olsson, *Phys. Rev. Lett.* **2004**, 93, 145901.
- [6] H. A. Zambrano, J. H. Walther, P. Koumoutsakos, I. F. Sbalzarín, *Nano Lett.* **2009**, 9, 66.
- [7] B. M. Kim, S. Qian, H. H. Bau, *Nano Lett.* **2005**, 5, 873.
- [8] J. H. Warner, Y. Ito, M. H. Rummeli, B. Büchner, H. Shinohara, G. A. D. Briggs, *ACS Nano* **2009**, 3, 3037.
- [9] Y. Gao, Y. Bando, *Nature* **2002**, 415, 599.
- [10] P. S. Dorozhkin, S. V. Tovstonog, D. Golberg, J. Zhan, Y. Ishikawa, M. Shiozawa, H. Nakanishi, K. Nakata, Y. Bando, *Small* **2005**, 1, 1088.
- [11] D. Golberg, P. M. F. J. Costa, M. Mitome, S. Hampel, D. Haase, C. Mueller, A. Leonhardt, Y. Bando, *Adv. Mater.* **2007**, 19, 1937.
- [12] G. E. Begtrup, W. Gannett, T. D. Yuzvinsky, V. H. Crespi, A. Zettl, *Nano Lett.* **2009**, 9, 1835.
- [13] K. Kim, K. Jensen, A. Zettl, *Nano Lett.* **2009**, 9, 3209.
- [14] L. Jankovič, D. Gournis, P. N. Trikalitis, I. Arfaoui, T. Cren, P. Rudolf, M. H. Sage, T. T. M. Palstra, B. Kooi, J. D. Hosson, M. A. Karakassides, K. Dimos, A. Moukarika, T. Bakas, *Nano Lett.* **2006**, 6, 1131.
- [15] F. Geng, H. Cong, *Phys. B* **2006**, 382, 300.
- [16] Q. Zhang, W. Z. Qian, H. Yu, F. Wei, Q. Wen, *Appl. Phys. A* **2007**, 86, 265.
- [17] G. Y. Zhang, E. G. Wang, *Appl. Phys. Lett.* **2003**, 82, 1926.
- [18] G. Du, W. Li, Y. Liu, *J. Phys. Chem. C* **2008**, 112, 1890.
- [19] D. Schebarchov, S. C. Hendy, *Nano Lett.* **2008**, 8, 2253.
- [20] D. Schebarchov, S. C. Hendy, *Phys. Rev. E* **2008**, 78, 046309.
- [21] K. Edgar, S. C. Hendy, D. Schebarchov, R. D. Tilley, *Small* **2011**, 7, 737.

- [22] S. Ozawa, K. Morohoshi, T. Hibiya, H. Fukuyama, *J. Appl. Phys.* **2010**, *107*, 014910.
- [23] J. Zhao, J. Q. Huang, F. Wei, J. Zhu, *Nano Lett.* **2010**, *10*, 4309.
- [24] J. Y. Chen, A. Kutana, C. P. Collier, K. P. Giapis, *Science* **2005**, *310*, 1480.
- [25] B. J. Wiley, Z. Wang, J. Wei, Y. Yin, D. H. Cobden, Y. Xia, *Nano Lett.* **2006**, *6*, 2273.
- [26] J. Lee, T. Tanaka, K. Seo, N. Hirai, J. G. Lee, H. Mori, *Rare Metals* **2006**, *25*, 469.
- [27] V. C. Holmberg, M. G. Panthani, B. A. Korgel, *Science* **2009**, *326*, 405.
- [28] G. R. Willmott, C. Neto, S. C. Hendy, *Faraday Discuss.* **2010**, *146*, 233.
- [29] A. Kutana, K. P. Giapis, *Phys. Rev. B* **2007**, *76*, 195444.
- [30] Y. C. Chang, Y. H. Liaw, Y. S. Huang, T. Hsu, C. S. Chang, T. T. Tsong, *Small* **2008**, *4*, 2195.
- [31] J. Y. Huang, S. Chen, S. H. Jo, Z. Wang, D. X. Han, G. Chen, M. S. Dresselhaus, Z. F. Ren, *Phys. Rev. Lett.* **2005**, *94*, 236802.
- [32] M. C. Wu, C. L. Li, C. K. Hu, Y. C. Chang, Y. H. Liaw, L. W. Huang, C. S. Chang, T. T. Tsong, T. Hsu, *Phys. Rev. B* **2006**, *74*, 125424.

Received: February 19, 2012
Published online: